Transient Development of Perturbations in Stratified Shear Flow

BRIAN F. FARRELL

Department of Earth and Planetary Sciences, Harvard University, Cambridge, Massachusetts

PETROS J. IOANNOU

Center for Meteorology and Physical Oceanography, Massachusetts Institute of Technology, Cambridge, Massachusetts

(Manuscript received 15 April 1992, in final form 23 October 1992)

ABSTRACT

Transient development of perturbations in inviscid stratified shear flow is investigated. Use is made of closed form analytic solutions that allow concise identification of optimally growing plane-wave solutions for the case of an unbounded flow with constant shear and stratification. For the case of channel flow, variational techniques are employed to determine the optimally growing disturbances.

The maximum energy growth attained over a specific time interval decreases continuously with increasing stratification, and no special significance attaches to Ri = 0.25. Indeed, transient growth can be substantial even for Ri = O(1). A general lower bound on the energy growth attained by an optimal perturbation in a stratified flow over a given time interval is the square root of the growth attained by the corresponding perturbation in unstratified flow. Enhanced perturbation persistence is found for mean-flow stratification lying in the range $0.1 < \mathrm{Ri} < 0.3$. Small but finite perturbations in mean flow with $\mathrm{Ri} < 0.4$ produce regions with locally negative total density gradient, which are expected to overturn. Although the perturbations are of wave form, buoyancy fluxes mediate transfer between perturbation kinetic and potential energy during transient development, thus implying that buoyancy flux is not a determinative diagnostic for distinguishing between waves and turbulence in stratified flows.

1. Introduction

One of the most striking features of atmospheric and oceanic flows is that they are commonly and characteristically stably stratified. The stratosphere, the midtroposphere, and often the planetary boundary layer are stably stratified. Similarly in the ocean, only episodically does the upper oceanic layer develop unstable stratification. This nearly ubiquitous stable stratification of geophysical flows distinguishes these flows from their laboratory counterparts from which buoyancy effects are usually absent.

Stratification supports internal gravity oscillations that pervade the atmosphere and the ocean, and much theoretical and observational work has been devoted to understanding the origin and effect of these waves. Regarding their origin, topographic forcing received early attention (Queney 1948; Scorer 1949, 1955; Long 1953; Nastrom and Fritts 1992), while observations and theory of gravity-wave excitation in shear zones, fronts, and convective elements have been the subject of recent study (Stull 1976; Fritts 1982; Fritts and Nastrom 1992). In the ocean, wave–wave interactions are thought to scatter internal gravity waves to produce the background internal-wave spectrum identified by Garrett and Munk (1979).

The effect on mean flows of momentum transported by gravity waves was an early theoretical prototype for wave–mean flow interaction. Theoretical work by Eliassen and Palm (1961) and Bretherton (1969) set the stage for subsequent extensions. The significance of topographic wave drag and associated momentum deposition high in the atmosphere was recognized by Sawyer (1959) and Lilly (1972). The importance of gravity waves for the general circulation of the stratosphere and mesosphere is well established. Breaking of gravity waves in the upper atmosphere, where wave amplitude increase with height as $[\rho_0(z)]^{-1/2}$, ρ_0 being the mean density, is a source of turbulence in the mesosphere that has been related to the observed reversal of pole to pole temperature gradient at the mesopause (Lindzen 1990). Wave–mean flow interaction theory was significantly advanced by the work of Booker and Bretherton (1967), who investigated the effect of critical layers on the propagation of gravity waves. They showed that a critical layer located in a stratified shear flow with local Richardson number (the ratio of local Brunt–Väisälä frequency to square shear) greater than one-quarter absorbed wave energy and that the critical layer is the location of wave-momentum exchange with the mean flow.

Corresponding author address: Dr. Brian F. Farrell, Department of Earth and Planetary Sciences, Pierce Hall, Harvard University, Cambridge, MA 02138.

The importance of the Richardson number for the maintenance of turbulence was recognized by Richardson (1920) and Taylor (1931a). By demanding that during turbulent exchange the work done against the gravitational field does not exceed the kinetic energy available in the sheared flow, they obtained Ri < 1 as a necessary condition for the maintenance of turbulence. Prandtl (1942), independently, reached the same conclusions using mixing-length theory. More recently, Chandrasekhar (1961) presented a budget argument that seemed to tighten the bound for the existence of turbulence to Ri = 0.25, apparently in compelling agreement with the the results of linearized stability analysis, but Miles (1986) reconsidered Chandrasekhar's calculation and confirmed the previous results of Richardson (1920), Taylor (1931a), and Prandtl (1942). The stability problem of inviscid stratified flows was formulated by Taylor (1931b) and Goldstein (1931), who also investigated the significance of the Richardson number for the existence of exponentially growing solutions, but it was not until the work of Miles (1961) and Howard (1961) that the importance of the Richardson number for the existence of modal instabilities was established. They found that a necessary condition for the presence of exponentially growing modes in inviscid stratified flows is that Ri < 0.25 somewhere in the flow. While the theorem of Miles and Howard provides a necessary condition for inviscid modal instability, it was realized by Taylor (1931b) and Goldstein (1931) that stratified Couette flow is a counterexample to the sufficiency of the theorem for instability. The preeminence of modal-instability thinking led investigators to identify Ri = 0.25 as the boundary between turbulent and laminar flow, despite the caution of Taylor (1931a):

". . . *though all infinitely small motions in a fluid seem to be stable when* Ri > 0.25, *this does not mean that all cases of flow for which* Ri > 0.25 *are non-turbulent. The steady flow of a viscous fluid through a pipe is apparently absolutely stable for infinitely small disturbances at all speeds, but it is well known that if the speeds exceed a certain limit the motion becomes turbulent.*"

While observations of turbulence give some support to sufficiency in practice of the Miles and Howard theorem, with breakdown commonly occurring for Ri ≈ 0.25, strict adherence to the Ri = 0.25 criterion is not observed and generally turbulence is present for Ri < 1 (Woods 1969). In this paper, optimal perturbations are obtained that demonstrate growth for all Ri.

Although much progress has been made toward understanding the excitation of gravity waves and the interaction between gravity waves and their background flow, many questions remain. Observations of turbulence in geophysical flows show that in the presence of stratification, turbulence is highly intermittent and organized in local regions of convective overturning frequently called "patches." Moreover turbulence in stratified flows does not seem to follow straightforward interpretation of the paradigm of Kolmogoroff for unstratified flows, according to which a fully developed statistical state produces an energy spectrum in agreement with similarity theory (Turner 1979). Microstructure in stratified flows seems rather to result from early decay of transitional structures that collapse convectively before maturing into turbulence (Thorpe 1987). Identification of processes that lead to local convective overturning in stratified flow assumes special importance in light of these observations. While most of the processes already cited, including wave–wave interaction, critical layer absorption, and exponentially growing instability, can lead under favorable circumstances to convective overturning, in this study we will investigate the transient development of perturbations in stratified flow and show that with initial perturbation energy exceeding approximately 1% of the background energy density, regions of local overturning arise rapidly for Ri < 0.4. This process takes place in Boussinesq flows that do not exhibit wave-amplitude increase due to variation in background density and have no exponential growing modes.

Recent theoretical work on the initial development of perturbations in shear flows (Farrell 1984, 1988a,b) has demonstrated that the nonorthogonality of the modal spectrum can account for rapid energy amplification of properly configured disturbances even for flows that do not support exponential modal instabilities. Emphasis on early development of forced disturbances arises naturally from this initial value approach, and a powerful variational method for determining the optimally growing initial conditions has been advanced that can lead to a full characterization of the stability properties of a shear flow (Farrell 1988a,b). In this study, we concentrate on transient development and on finding optimal disturbances in inviscid stratified flow, first making use of closed form solutions valid for unbounded constant shear and then applying matrix variational methods to study stratified channel flow.

2. Formulation

Consider a Boussinesq fluid with density:

$$\rho(x, z, t) = \rho_m + \rho_0(z) + \rho'(x, z, t), \quad (2.1)$$

where ρ_m is the mean, $\rho_0(z)$ is the space variation of the background density that is confined to vary only in the vertical coordinate z, and ρ' is the density fluctuation. The pressure p is similarly decomposed. Consider evolution of disturbances superposed on a flow with velocity in the x direction, $U(z)$, and steady-state pressure and density related by

$$\frac{dp_0}{dz} = -g(\rho_m + \rho_0). \quad (2.2)$$

The linearized equations governing the inviscid evolution of disturbances on this background state satisfy the following equations:

$$(\partial_t + U\partial_x)u + \frac{dU}{dz}w = -\frac{1}{\rho_m}\partial_x p', \tag{2.3}$$

$$(\partial_t + U\partial_x)w = -\frac{1}{\rho_m}\partial_z p' - g\frac{\rho'}{\rho_m}, \tag{2.4}$$

$$(\partial_t + U\partial_x)\rho' + w\frac{d\rho_0}{dz} = 0, \tag{2.5}$$

$$\partial_x u + \partial_z w = 0, \tag{2.6}$$

where u is the perturbation x velocity, w is the perturbation z velocity, and g is the gravitational acceleration. The divergenceless perturbation velocity field can be expressed in terms of a streamfunction as $(u, w) = (-\psi_z, \psi_x)$.

We will consider a constant shear velocity profile $U = \alpha z$, with $\alpha > 0$ for definiteness, and nondimensionalize time by the shear, $t = \tilde{t}/\alpha$, and the horizontal and vertical scales by $L = U_0/\alpha$, where U_0 may be chosen, for example, to be a typical background velocity in the atmospheric boundary layer. Pressure and density are nondimensionalized by $p' = \rho_m U_0^2 \tilde{p}$ and $\rho' = \rho_m(U_0 N_0^2/\alpha g)\tilde{\rho}$, respectively, where $N^2 = -(g/\rho_m)(d\rho_0/dz)$ is the Brunt–Väisälä frequency and N_0 is a typical value of this frequency in the domain of the flow. Only cases of stable mean stratification for which $N^2 > 0$ will be considered. After dropping tildes, the nondimensional equations take the form:

$$(\partial_t + z\partial_x)u + w = -\partial_x p, \tag{2.7}$$

$$(\partial_t + z\partial_x)w = -\partial_z p - \mathrm{Ri}\rho, \tag{2.8}$$

$$(\partial_t + z\partial_x)\rho - \frac{N^2}{N_0^2}w = 0, \tag{2.9}$$

$$\partial_x u + \partial_z w = 0, \tag{2.10}$$

where the Richardson number $\mathrm{Ri} \equiv N_0^2/\alpha^2$ is a measure of the relative strength of the stratification and shear of the background flow. In terms of the streamfunction ψ (2.7)–(2.10) can be written equivalently as

$$(\partial_t + z\partial_x)\nabla^2\psi = -\mathrm{Ri}\partial_x\rho, \tag{2.11}$$

$$(\partial_t + z\partial_x)\rho = \frac{N^2}{N_0^2}\partial_x\psi. \tag{2.12}$$

The boundary condition requires zero vertical velocity at horizontal boundaries, which implies vanishing of the perturbation density at these boundaries.

It should be noted that in the derivation of (2.11) and (2.12), the effects of dissipation and diffusion are neglected and only two-dimensional disturbances are considered. Our concern lies with initial development of these disturbances and not with their large-time asymptotic behavior. Comparison of the inviscid dynamics to the dynamics with diffusion (Criminale and Cordova 1986) shows that for the first stages of development the diffusive effects can be neglected, but that at later times diffusive effects must be taken into account.

In order to determine a disturbance, the distribution of both the streamfunction ψ and buoyancy ρ needs to be specified. If the initial perturbation buoyancy is zero, one can say that the disturbance in the stratified flow is velocity forced, while if the initial velocity is zero, one can say that the flow is buoyancy forced. Unlike unstratified flows, stratified flows have two degrees of freedom in the choice of initial conditions, reflecting the two forms of energy in stratified flows: potential and kinetic. It should also be noted that during transient development eddy potential energy and eddy kinetic energy are not necessarily equipartitioned.

The perturbation kinetic energy $T(t)$ is obtained by multiplying (2.4) by u and (2.5) by w, adding the resulting equations, and integrating over space to obtain

$$\frac{dT}{dt} = -\langle\overline{uw}\rangle - \mathrm{Ri}\langle\overline{\rho w}\rangle, \tag{2.13}$$

where the overbar signifies an x average, brackets signify a z average, and

$$T = \left\langle\frac{\overline{u^2 + w^2}}{2}\right\rangle. \tag{2.14}$$

The perturbation potential energy $V(t)$ is obtained by multiplying (2.6) by $\mathrm{Ri}(N_0^2/N^2)\rho$:

$$\frac{dV}{dt} = \mathrm{Ri}\,\langle\overline{\rho w}\rangle, \tag{2.15}$$

where

$$V = \left\langle\mathrm{Ri}\frac{N_0^2}{N^2}\frac{\overline{\rho^2}}{2}\right\rangle. \tag{2.16}$$

Variation of the total perturbation energy density per unit mass $E(t)$ is obtained by adding (2.13) and (2.15):

$$\frac{dE}{dt} = -\langle\overline{uw}\rangle. \tag{2.17}$$

Changes in perturbation energy are related solely to the downgradient Reynolds stress $\overline{uw}$, exactly as in an unstratified flow. This shows that the only source of energy for the perturbations is the mean shear. Normal-mode solutions of (2.11) and (2.12) have density and vertical velocity in quadrature leading to zero buoyancy flux $\overline{\rho w}$ and equipartition of energy between kinetic and potential forms. During transient development, the buoyancy flux is nonzero, leading to transformations between the two forms of energy. From (2.13) and (2.15) we note that the buoyancy flux $\overline{\rho w}$ does not contribute to the total energy but rather participates in redistribution of energy between its kinetic and potential forms.

3. Development of disturbances in an unbounded flow with constant shear

Remarkably, in the case of an unbounded flow with constant shear and constant N^2, (2.11) and (2.12) admit closed-form solutions (Phillips 1966; Hartman 1975), which can be obtained by transforming to convected coordinates,

$$\xi = x - zt, \quad \eta = z, \quad \tau = t, \tag{3.1}$$

so that (2.11) and (2.12) become

$$\partial_\tau[\partial_\xi^2 + (\partial_\eta - \tau\partial_\xi)^2]\psi = -\mathrm{Ri}\partial_\xi\rho, \tag{3.2}$$

$$\partial_\tau\rho = \partial_\xi\psi. \tag{3.3}$$

In these convected coordinates, (3.2) and (3.3) are separable in ξ and η, and it is sufficient to determine the evolution of a single Fourier component that can be written alternatively in the convected and laboratory frame:

$$\psi = \hat{\psi}(\tau)e^{i(k\xi+l\eta)} = \hat{\psi}(\tau)e^{i[kx+(l-kt)z]}, \tag{3.4a}$$

$$\rho = \hat{\rho}(\tau)e^{i(k\xi+l\eta)} = \hat{\rho}(\tau)e^{i[kx+(l-kt)z]}, \tag{3.4b}$$

in which the real parts are interpreted as the physical solution. Note that in the laboratory frame (x, z), the plane-wave solutions of (3.2) and (3.3) have time-varying vertical wavenumber. In the sequel, when the plane wave is referred to with wavenumber (k, l), what is meant is the plane wave that in the laboratory frame has this wavenumber at $t = 0$, with the understanding that at a later time the vertical wavenumber is $l - kt$. Note that each Fourier component (k, l) is also a nonlinear solution in isolation but not in superposition. To determine the evolution of the complex amplitudes $\hat{\psi}$ and $\hat{\rho}$ for a plane wave with wavenumber (k, l), we introduce (3.4) into (3.2) and (3.3) to obtain

$$\frac{d}{d\tau}[k^2 + (l - k\tau)^2]\hat{\psi} = ik\,\mathrm{Ri}\hat{\rho}, \tag{3.5}$$

$$\frac{d\hat{\rho}}{d\tau} = ik\hat{\psi}. \tag{3.6}$$

Equations (3.5) and (3.6) can be combined to get

$$\frac{d^2\hat{\zeta}}{d\tau^2} + \frac{\mathrm{Ri}}{1 + (\sigma - \tau)^2}\hat{\zeta} = 0, \tag{3.7}$$

where

$$\hat{\zeta} = [1 + (\sigma - \tau)^2]\hat{\psi} \tag{3.8}$$

is proportional to the vorticity, and $\sigma = l/k$ is a measure of the initial tilt of the wave. The solution of this equation can be formally expressed using hypergeometric functions (Hartman 1975), and it can be accurately determined by numerical integration. Specification of the initial values of buoyancy and streamfunction for each Fourier component determines the evolution of an arbitrary composite physical disturbance.

The energy density equation (2.17) can be written as

$$\frac{dE}{d\tau} = \frac{k^2}{2}(\sigma - \tau)|\hat{\psi}|^2. \tag{3.9}$$

For $\sigma > 0$, the wave is configured to produce Reynolds stress down the mean momentum gradient of the background flow and the energy grows until $t_v = \sigma$, at which time the wave has zero vertical wavenumber in the laboratory frame and the energy density assumes its maximum value. At later times, the energy decays. To determine the rate of decay according to inviscid dynamics, note that for large times the differential equation (3.7) can be approximated by

$$\frac{d^2\hat{\zeta}}{d\tau^2} + \frac{\mathrm{Ri}}{\tau^2}\hat{\zeta} = 0. \tag{3.10}$$

This can be readily solved to give, consistent with Brown and Stewartson (1980), the asymptotic dependence

$$\hat{\psi} \approx \tau^{-(3/2)\pm\nu}, \tag{3.11a}$$

$$\hat{\rho} \approx \tau^{-(1/2)\pm\nu}, \tag{3.11b}$$

leading to an energy decay,

$$E \approx \tau^{-1\pm2\nu}, \tag{3.11c}$$

where $\nu = (0.25 - \mathrm{Ri})^{1/2}$. It is worth noting that the energy decays as $E \approx \tau^{-2\mathrm{Ri}}$ for small Ri. Note also that although for $\mathrm{Ri} > 0.25$ the solutions are asymptotically oscillatory, the rapid energy decay allows only $O(\nu)$ complete cycles to occur. Consequently, the asymptotic oscillatory behavior is not evident unless $\mathrm{Ri} \gg 1$ (Hartman 1975). In an unstratified flow, the energy decays as $E \approx \tau^{-2}$, revealing that the $\mathrm{Ri} \to 0$ limit is nonuniform for inviscid dynamics.

It is instructive to consider separately the limits of small and large Ri. The small Ri expansion of the hypergeometric solutions of (3.7) give, for a plane wave with $\sigma = l/k$ at $t = 0$ and for times of $o(\mathrm{Ri}^{-1})$,

$$\hat{\zeta} = \hat{\zeta}_0, \tag{3.12a}$$

$$\hat{\rho} = k\hat{\zeta}_0[\tan^{-1}(t - \sigma) + \tan^{-1}\sigma] + \hat{\rho}_0, \tag{3.12b}$$

where $k^2\hat{\zeta}_0$ and $\hat{\rho}_0$ are the initial real value of vorticity and imaginary value of buoyancy, respectively. For small Ri and small times, the vorticity is conserved and the density is advected as if it were a passive tracer. Kinetic energy is transferred into potential energy on the advective time scale subsequent to which there is decay of the total energy on a time scale $o(\mathrm{Ri}^{-1})$. For small Ri, the buoyancy fluctuations are expected to become large and, consistent with (3.11c), long lived. This conversion of kinetic energy to potential energy at the early stages of the development may give rise, even for small initial perturbations, to regions with perturbation density gradient larger than the ambient

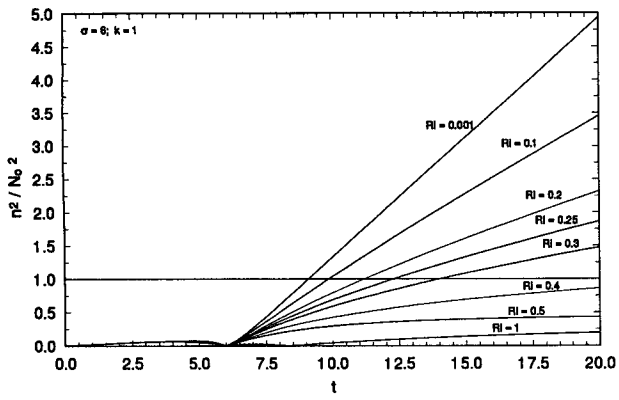

FIG. 1. Evolution of the maximum perturbation density gradient measured by $n^2 = |(g/\rho_m)\partial\rho/\partial z|$ normalized by the background Brunt-Väisälä frequency N_0^2 as a function of time for various Ri in an unbounded shear flow. The curves show actual integrations and are not based on the asymptotic results presented. The disturbance at $t = 0$ is a plane wave with $k = 1$ and $l = 6$, with no initial buoyancy perturbation, and the initial energy is 1% of the background energy density. When $n^2/N_0^2 > 1$, the disturbance is expected to develop secondary instabilities of the Rayleigh-Taylor type and to overturn creating regions of local turbulence.

density gradient. In these regions, the total density gradient becomes locally negative and secondary instabilities of the Rayleigh-Taylor type can plausibly be expected to occur, producing rapid overturning and the formation of local regions of turbulence. A typical evolution of perturbation density gradient is shown as a function of time for various Ri in Fig. 1. The initial perturbation has the form of a plane wave with $k = 1$ and $l = 6$. It is excited with zero density perturbation and with energy density 1% of the background energy density. The calculations presented in Fig. 1 are not based on the asymptotic approximations presented but rather on the full solution of (3.7). It is remarkable that breaking is expected to occur within a few advective time units when $\mathrm{Ri} < 0.4$, while for larger Ri breaking is considerably delayed. Different initial conditions show this behavior to be robust. It appears likely that this abrupt increase in the susceptibility of the flow to overturning for $\mathrm{Ri} < 0.4$ may account for observations of convective saturation of stratified flow disturbances at comparable Ri (Hopfinger 1973).

For large Ri, WKB analysis can be applied to (3.7). Recall the WKB solution to the differential equation,

$$\frac{d^2y}{dt^2} + \lambda f(t) y = 0, \tag{3.13}$$

where λ is a large parameter:

$$y(t) = \frac{1}{[f(t)]^{1/4}} \exp\left\{\pm\lambda^{1/2}\int^t [f(\tau)]^{1/2} d\tau\right\}. \tag{3.14}$$

This solution to $O(\lambda^{-1/2})$ is valid when

$$\left|\frac{f'}{2f^{1/2}}\right| \ll \lambda^{1/2}|f|. \tag{3.15}$$

Applying WKB analysis in (3.7), the solution to $O(1/\mathrm{Ri}^{1/2})$ is obtained for a plane wave with initial complex amplitudes $\hat{\xi}_0$, $\hat{\rho}_0$:

$$\hat{\xi} = \frac{f_0^{1/4}}{f^{1/4}}\left(\hat{\xi}_0\cos\phi + \frac{i\,\mathrm{Ri}^{1/2}}{k f_0^{1/2}}\hat{\rho}_0\sin\phi\right), \tag{3.16a}$$

$$\hat{\rho} = \frac{ikf^{1/4}}{\mathrm{Ri}^{1/2}}\left(\hat{\xi}_0 f_0^{1/4}\sin\phi - \frac{i\,\mathrm{Ri}^{1/2}}{k f_0^{1/4}}\hat{\rho}_0\cos\phi\right), \tag{3.16b}$$

where $f \equiv f(t) = [1 + (t-\sigma)^2]^{-1}$, $f_0 \equiv f(0)$, and $\phi \equiv \mathrm{Ri}^{1/2}\int_0^t f^{1/2}$. The energy density $E(t)$ is given by

$$E(t) = \frac{f^{1/2}}{2}\left(k^2 f_0^{1/2}|\hat{\xi}_0|^2 + \mathrm{Ri}\,\frac{|\hat{\rho}_0|^2}{f_0^{1/2}}\right), \tag{3.17}$$

leading to an energy amplification

$$\frac{E(t)}{E(0)} = \left[\frac{E_0(t)}{E_0(0)}\right]^{1/2}, \tag{3.18}$$

where

$$\frac{E_0(t)}{E_0(0)} = \frac{1+\sigma^2}{1+(\sigma-t)^2} \tag{3.19}$$

is the amplification for $\mathrm{Ri} = 0$. According to this order of WKB theory, the energy amplification for large Ri is independent of the Richardson number and equal to the square root of the energy amplification for unstratified flow. Although WKB theory to $O(1/\mathrm{Ri}^{1/2})$ predicts monotonic decay of energy density for all times $t > \sigma$, the actual solution, even for high Ri, leads to oscillations of the energy decay about the WKB energy decay curve (cf., the Appendix).

4. Optimal excitation of unbounded stratified constant shear flow

The evolution of a plane-wave perturbation in an infinite stratified constant shear flow has been described. These perturbations require for their specification both an initial velocity and initial buoyancy. In a stochastically forced flow, it is likely that all initial conditions are excited, and consequently it is of interest to determine which of these initial conditions yield greatest energy growth in a specified time. The initial perturbation that maximizes energy growth over a specified interval of time T_{opt} will be called the optimal perturbation.

The plane-wave solutions developed in section 3 comprise an orthonormal basis in the inner product associated with either the L_2 or energy norm. A general initial perturbation can be considered as a Fourier superposition of plane waves, and, because of the orthogonality property, determination of the optimal

perturbation reduces to determination of the optimal perturbation from the class of single plane waves. Having chosen the optimizing time T_{opt} and the Richardson number Ri determination of the optimal perturbation reduces to a search for $(\sigma = l/k, \hat{\psi}_0, \hat{\rho}_0)$, which specify the initial perturbation that maximizes the energy density growth:

$$G(T_{opt}, \mathrm{Ri}) = \frac{E(\sigma, \hat{\psi}_0, \hat{\rho}_0; T_{opt}, \mathrm{Ri})}{E(\sigma, \hat{\psi}_0, \hat{\rho}_0; 0, \mathrm{Ri})}, \quad (4.1)$$

with the energy density E determined from (3.9). The optimal plane-wave perturbation is found by means of a conjugate gradient optimization algorithm. The dependence of the maximum energy growth G on the optimizing time T_{opt} and Ri is shown in Fig. 2. For small T_{opt}, the maximum energy density growth obtained is independent of Ri. The energy tendency (2.17) depends only on the perturbation velocity correlation, implying that for small enough times, all perturbations with the same velocity structure will produce the same growth independent of Ri. This consideration further implies that the maximum growth rate $d[\ln(G)]/dt \to 1$ for $T_{opt} \to 0$, with time nondimensionalized by the shear, again independent of Ri. This maximum growth rate is the same as the energy growth rate for an unstratified flow found using energy methods (Joseph 1976). Note in Fig. 2 the gradual decrease of the maximum energy growth $G(T_{opt}, \mathrm{Ri})$ with increasing Ri. For large T_{opt} and large Ri, the decrease of the maximum energy growth G is not monotonic with increasing Ri. These oscillations imposed on the energy decay are seen in the full solutions, but they are not captured in the WKB approximations (cf., the Appendix).

While T_{opt} is arbitrary in this model problem, in practice ambient turbulent fluctuations impose a time scale over which the growth of perturbations is limited due to disruption of their coherent motion. This time scale is often taken to be the eddy turnover time. A representative value $T_{opt} = 6$ has been selected for study. This value, although conservative, demonstrates the potential of transient growth in stratified shear flows. Different choices for T_{opt} do not change the qualitative results obtained. The development of the total energy density, kinetic energy density, and potential energy density as a function of time is shown for $T_{opt} = 6$ in Fig. 3, Fig. 4, and Fig. 5, respectively. The optimal disturbance involves some buoyancy forcing with such a phase relative to that of the velocity perturbation that during the first stages of the development the buoyancy flux is negative and tends to reinforce the kinetic energy of the disturbance. The ratio of initial potential energy to total energy is tabulated in Table 1. The buoyancy flux as a function of time for various Ri is shown in Fig. 6. During the period of maximum energy amplification, the buoyancy flux

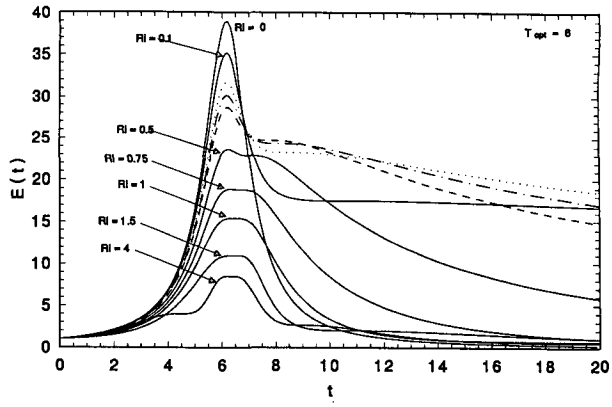

FIG. 3. Evolution of the perturbation total energy density of the optimal plane wave for $T_{opt} = 6$ as a function of time for various Ri in an unbounded shear flow. The dotted line corresponds to Ri = 0.2. The dot–dash line to Ri = 0.25 and the dashed line to Ri = 0.3. For comparison, the energy variation for the case of no stratification (Ri = 0) is included.

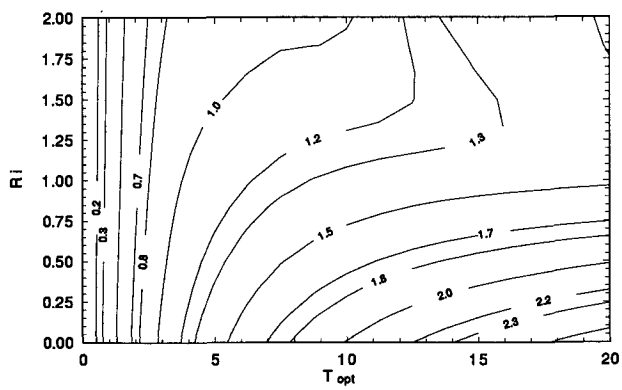

FIG. 2. Maximum energy growth G of optimal perturbations as a function of optimizing time T_{opt} and Ri. The contour values of G are logarithmic (with base 10).

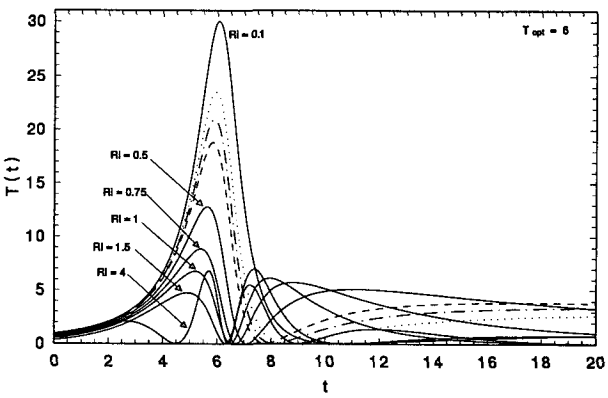

FIG. 4. Evolution of the perturbation kinetic energy density of the optimal plane wave for $T_{opt} = 6$ as a function of time for various Ri in an unbounded shear flow. The dotted line corresponds to Ri = 0.2. The dot–dash line to Ri = 0.25 and the dashed line to Ri = 0.3.

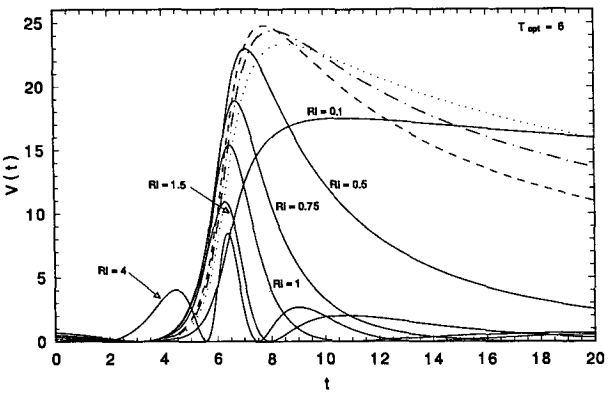

FIG. 5. Evolution of the perturbation potential energy density of the optimal plane wave for $T_{opt} = 6$ as a function of time for various Ri in an unbounded shear flow. The dotted line corresponds to Ri = 0.2. The dot–dash line to Ri = 0.25, and the dashed line to Ri = 0.3.

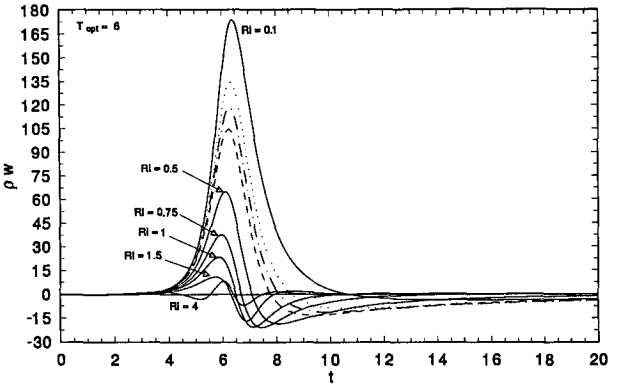

FIG. 6. Evolution of the buoyancy flux $\overline{\rho w}$ of the optimal plane wave for $T_{opt} = 6$ as a function of time for various Ri in an unbounded shear flow. The dotted line corresponds to Ri = 0.2. The dot–dash line to Ri = 0.25 and the dashed line to Ri = 0.3.

is positive for every Ri, which reduces the growth of kinetic energy. As a result, the optimals in a stratified flow have smaller maximum growth than their counterparts in unstratified flows.

It can be seen from Fig. 3 that there is enhanced persistence of total energy for values of Ri approximately in the range $0.1 < \mathrm{Ri} < 0.3$. Such enhanced persistence has important implications for maintenance of variance in stochastically forced flows (Farrell and Ioannou 1993) with enhanced perturbation variance expected for $0.1 < \mathrm{Ri} < 0.3$. However, the increased susceptibility of flows in this Ri regime to convective overturning, as remarked earlier, can be expected to considerably complicate interpretation of observations in this physically interesting region of parameter space.

5. Optimal excitation of bounded stratified constant shear flow

Consider a constant shear flow with fixed N^2 in a channel $|z| \leq 0.5$. Perturbations evolve according to (2.11) and (2.12), and the initial conditions that will attain the greatest energy amplification at a specified later time T_{opt} can be determined using a variational method (Farrell 1988a,b). Consider solutions of (2.11) and (2.12) of the form

$$\psi = \hat{\psi}(z)e^{ik(x-ct)}, \tag{5.1a}$$

$$\rho = \hat{\rho}(z)e^{ik(x-ct)}, \tag{5.1b}$$

in which only the real parts are interpreted as the physical solution. Substitution in (2.11) and (2.12) gives

$$z\Delta\hat{\psi} + \mathrm{Ri}\hat{\rho} = c\Delta\hat{\psi}, \tag{5.2}$$

$$z\hat{\rho} - \hat{\psi} = c\hat{\rho}, \tag{5.3}$$

where $\Delta = (d^2/dz^2) - k^2$. At the boundaries, $z = \pm 0.5$, $\hat{\psi} = 0$ is required. To determine the solutions, we solve the generalized eigenproblem, defined by (5.2) and (5.3) together with the boundary conditions, for the spectrum c and its associated eigenfunctions $(\hat{\psi}, \hat{\rho})$. The eigenfunctions form a complete set in terms of which any initial disturbance can be expressed. The constant shear flow does not support exponentially growing solutions of the form (5.1) for any $\mathrm{Ri} \geq 0$, that is, in (5.2) and (5.3) we have $\mathrm{Im}(c) = 0$ (Eliassen et al. 1953). The spectrum consists of a continuum with $-0.5 < c < 0.5$. When $\mathrm{Ri} > 0.25$, there is also a denumerable set of nonsingular neutral modes with phase speeds

$$\infty > |c_1| > \cdots > |c_n| \cdots > 0.5, \tag{5.4}$$

having ± 0.5 as a limit point (Dyson 1960; Kuo 1963).

From now on, the second-order finite-difference form of the differential operators appearing in (5.2) and (5.3) on a sufficiently high number N of mesh points will be considered, where any disturbance of interest can be adequately represented as

$$\hat{\psi}_s = \sum_{i=1}^{2N} \alpha_i \hat{\psi}_{i,s} e^{ik(x-c_i t)}, \tag{5.5a}$$

$$\hat{\rho}_s = \sum_{i=1}^{2N} \alpha_i \hat{\rho}_{i,s} e^{ik(x-c_i t)}. \tag{5.5b}$$

TABLE 1. Ratio of initial potential energy to total energy for the optimal plane wave for $T_{opt} = 6$ for various Ri.

Ri	$V(0)/E(0)$
0.10	0.06
0.20	0.12
0.25	0.15
0.30	0.18
0.50	0.29
0.75	0.42
1.00	0.53
1.50	0.69
4.00	0.36

Here the subscript s denotes the value at the sth mesh point ($1 \leq s \leq N$), c_i ($1 \leq i \leq 2N$) is the ith eigenvalue of the discretized version of the eigenvalue problem (5.2) and (5.3), $(\hat{\psi}_{i,s}, \hat{\rho}_{i,s})$ is the corresponding eigenfunction at the sth mesh point, and α_i are coefficients determined by the initial conditions. The accuracy of our numerical solutions was verified by doubling the resolution and obtaining negligible differences in the solutions over the time intervals studied.

The expression for the eddy energy at time t takes the discretized form

$$E^t = \frac{\delta}{4}\sum_{s=1}^{N}\left(\frac{d\hat{\psi}_s^*}{dz}\frac{d\hat{\psi}_s}{dz} + k^2\hat{\psi}_s^*\hat{\psi}_s + \mathrm{Ri}\hat{\rho}_s^*\hat{\rho}_s\right) = \sum_{i=1}^{2N}\sum_{j=1}^{2N} Y_{ij}^t a_i^* a_j, \quad (5.6)$$

where δ is the spacing of the mesh, * denotes complex conjugation, and

$$Y_{ij}^t = \frac{\delta}{4}\sum_{s=1}^{N}\left(\frac{d\hat{\psi}_{i,s}^*}{dz}\frac{d\hat{\psi}_{j,s}}{dz} + k^2\hat{\psi}_{i,s}^*\hat{\psi}_{j,s} + \mathrm{Ri}\hat{\rho}_{i,s}^*\hat{\rho}_{j,s}\right)e^{ik(c_i^*-c_j)t}. \quad (5.7)$$

The matrix $\mathbf{Y}_{ij}^t$ calculated at time t is denoted by $\mathbf{Y}^t$, and the $2N$-tuple $(\alpha_1, \cdots, \alpha_{2N})$ is denoted by α. Then the energy at time t takes the form

$$E^t = \alpha^*\mathbf{Y}^t\alpha, \quad (5.8)$$

in which the matrix $\mathbf{Y}^t$ is Hermitian and positive definite.

To determine the spectral projection α of the initial perturbation that maximizes E^t at the optimization time T_{opt} among all disturbances with unit initial energy E^0, the functional

$$F = E^{T_{\mathrm{opt}}} + \lambda(E^0 - 1) \quad (5.9)$$

is rendered stationary with respect to α, with λ a Lagrange multiplier. The initial condition α that renders this functional stationary satisfies the generalized eigenvalue problem

$$\mathbf{Y}^{T_{\mathrm{opt}}}\alpha + \lambda Y^0\alpha = 0. \quad (5.10)$$

The $2N$ eigenvalues λ_n determine the factor by which the energy at time t exceeds the initial energy when the initial disturbance is the corresponding eigenfunction α_n. Note that because $\mathbf{Y}^{T_{\mathrm{opt}}}$ is Hermitian and positive definite, the eigenvalues of (5.10), λ_n, are real and positive, and the corresponding orthonormal eigenfunctions α_n give the $2N$ directions of semimajor axes, each of length $\lambda_n^{1/2}$, of the eddy-energy-amplification ellipsoid (Farrell 1990). The volume of this ellipsoid in the absence of dissipation and diffusion is constant over time and proportional to $\prod_{n=1}^{n=2N}\lambda_n^{1/2}$. The α_n that corresponds to the maximum eigenvalue determines the optimum initial disturbance that gives the maximum energy amplification at time T_{opt}.

The eigenvalues λ_n for Ri = 0.1, 0.25, and 4 with k = 1 are shown in Fig. 7 for an optimizing time of six nondimensional time units. The modes that result in appreciable energy amplification are few; in this example, only three modes give amplification within 30% of the optimum, and this result is independent of discretization. One significant physical implication is that out of the continuum of initial conditions, a small number of disturbances are responsible for most of the growth, and therefore the effective dimensionality of the dynamics is in this sense much smaller than the numbers of degrees of freedom.

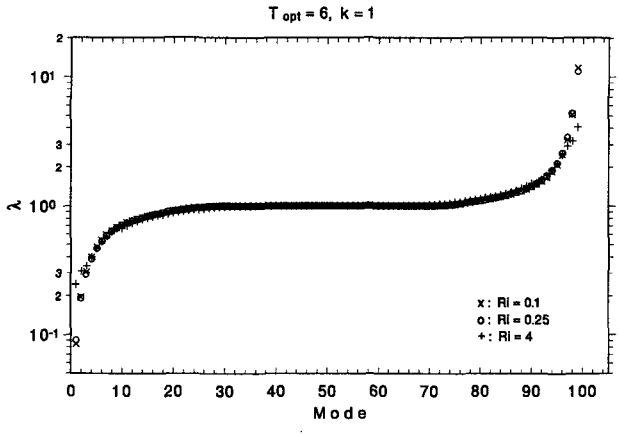

FIG. 7. Energy growth eigenvalues λ_n for various Ri for optimization time T_{opt} = 6 and k = 1 in a channel. Note that only the highest and lowest of the eigenvalues are affected by the variation of the Ri. The symmetry in this logarithmic plot reveals the invariance of the product of the eigenvalues, a consequence of the absence of dissipation and diffusion.

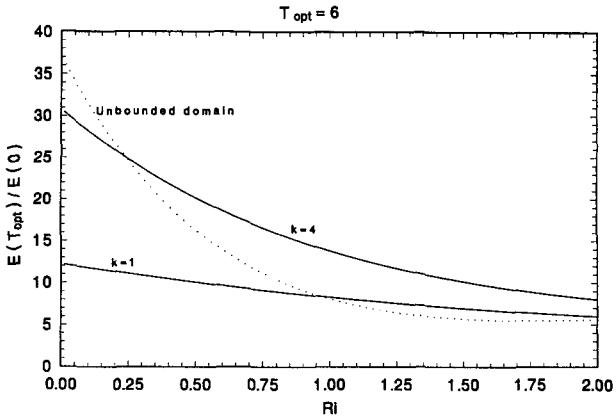

FIG. 8. Variation of the maximum energy for the optimum perturbation in a channel for T_{opt} = 6 as a function of Ri. The cases of k = 4 and k = 1 are shown. The dotted line is the maximum energy attained by the T_{opt} = 6 optimum plane wave in an unbounded flow.

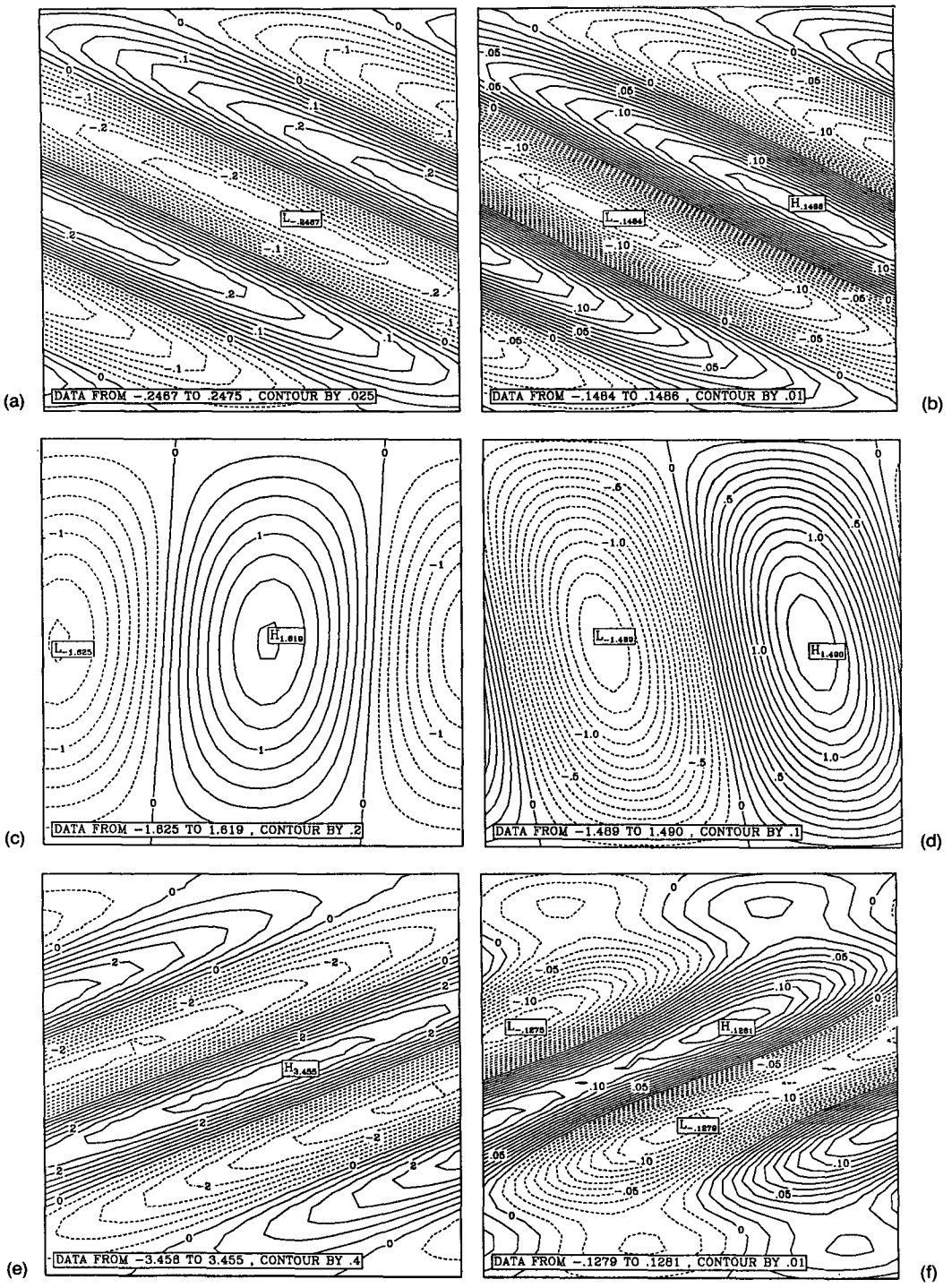

FIG. 9. Development of the optimal perturbation for Ri = 0.2 and T_{opt} = 6, k = 1 with initial energy, E = 1: (a) t = 0, the buoyancy perturbation (initial potential energy V comprises 6.9% of total energy); (b) t = 0, the streamfunction; (c) t = 6, the buoyancy perturbation (E = 10.84 and V = 22.2%); (d) t = 6, the streamfunction perturbation; (e) t = 15, the buoyancy perturbation (E = 12.91, V = 98.3%); (f) t = 15, the streamfunction perturbation.

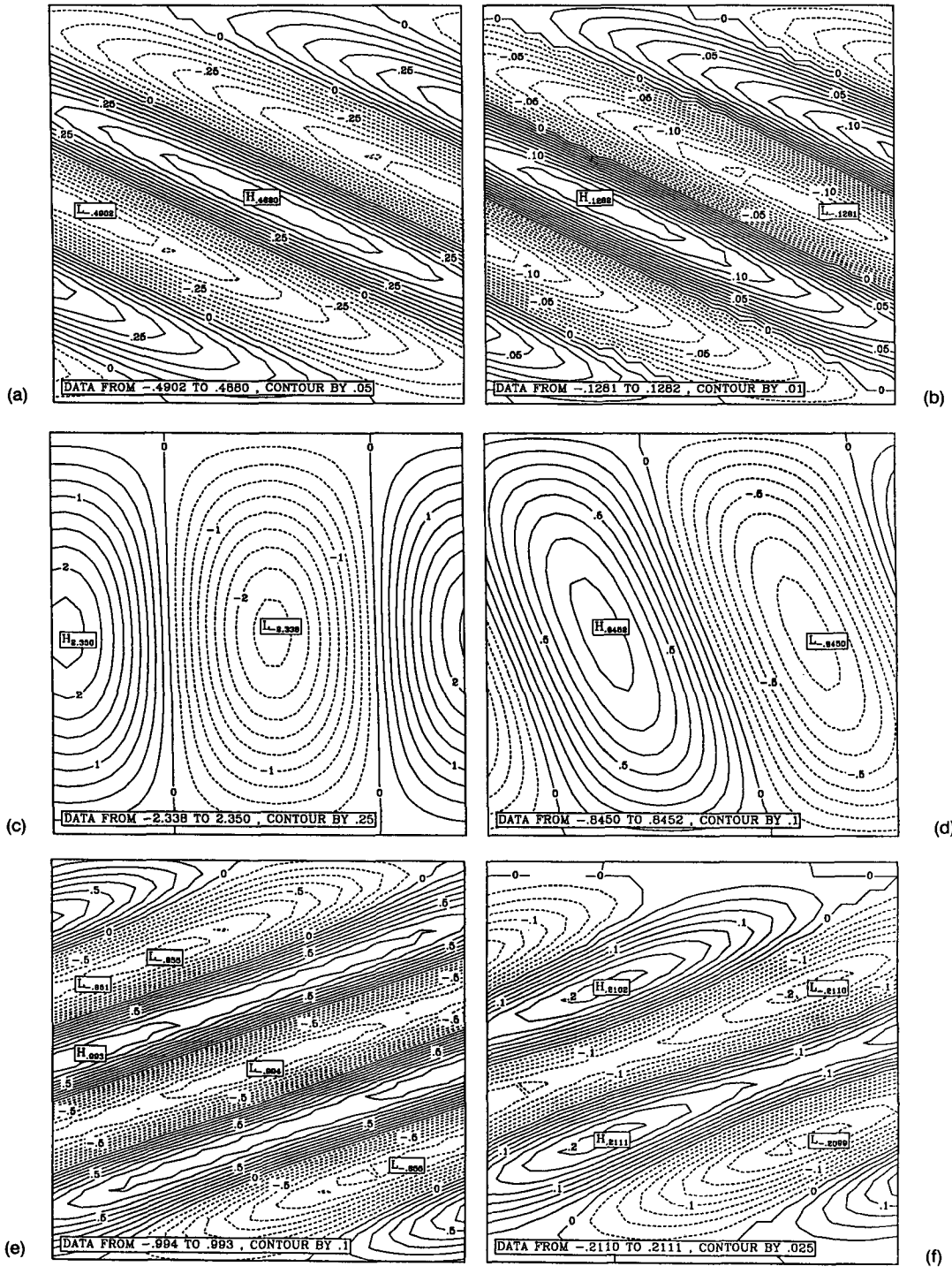

FIG. 10. Development of the optimal perturbation for Ri = 0.75 and $T_{opt} = 6$, $k = 1$ with initial energy, $E = 1$: (a) $t = 0$, the buoyancy perturbation (initial potential energy V comprises 25.3% of total energy); (b) $t = 0$, the streamfunction; (c) $t = 6$, the buoyancy perturbation ($E = 8.9$ and $V = 57.5\%$); (d) $t = 6$, the streamfunction perturbation; (e) $t = 15$, the buoyancy perturbation ($E = 6.5$, $V = 34.4\%$); (f) $t = 15$, the streamfunction perturbation.

TABLE 2. Ratio of initial potential energy to total energy for the optimal perturbation in a channel for $T_{opt} = 6$ for various Ri.

Ri	$V(0)/E(0)$
0.10	0.03
0.20	0.07
0.25	0.09
0.30	0.10
0.50	0.17
0.75	0.25
1.00	0.33
1.50	0.54
4.00	0.71

The maximum energy attained by the optimal perturbations as a function of Ri is shown in Fig. 8 for $k = 1$, 4, and optimizing time $T_{opt} = 6$. For reference, the result for the unbounded flow is also shown. The boundaries reduce the growth of the optimal perturbation in comparison with results for an unbounded flow. The optimal disturbances in the unbounded flow have an initial tilt such that $\sigma_{opt} = l/k \approx T_{opt}$. In bounded flow, large streamwise wavenumbers k associated with large vertical wavenumbers l are less influenced by the boundaries, and for these short wavelengths, the solutions in the bounded domain approach the solutions in the unbounded flow. This can be seen in Fig. 8 where the $k = 4$ growth is closer than the $k = 1$ growth to that of an unbounded flow. Further, note the smooth dependence of the maximal energy on Ri.

The structures of the optimal perturbations for $k = 1$, $T_{opt} = 6$, and Ri = 0.2, 0.75 are shown in Figs. 9 and 10. Initially, the growing perturbation streamfunction has the familiar tilt against the shear indicative of a downgradient Reynolds stress. The initial buoyancy perturbation is of the appropriate phase so that on average dense fluid descends while lighter fluid ascends, leading to kinetic energy increase. The optimal ratio of initial potential energy to total energy is tabulated in Table 2 for some representative choices of Ri.

The energy amplification of the optimally growing disturbance has been shown to only gradually decrease as the Ri increases. The development of total energy density, kinetic energy density, and potential energy density as a function of time are shown in Figs. 11–13, respectively, for $T_{opt} = 6$, $k = 1$, and various Ri. Note that there is enhanced persistence of the energy for $0.2 < Ri < 0.4$ because perturbations to flows in

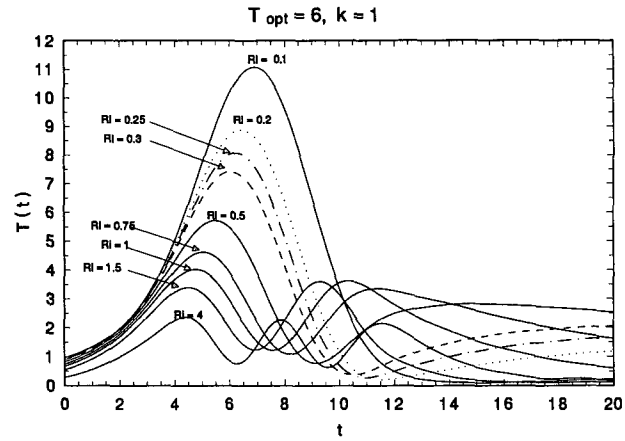

FIG. 12. Evolution of the perturbation kinetic energy density of the optimal perturbation in the channel for $T_{opt} = 6$ and $k = 1$ as a function of time for various Ri in an unbounded shear flow. The dotted line corresponds to Ri = 0.2. The dot–dash line to Ri = 0.25 and the dashed line to Ri = 0.3.

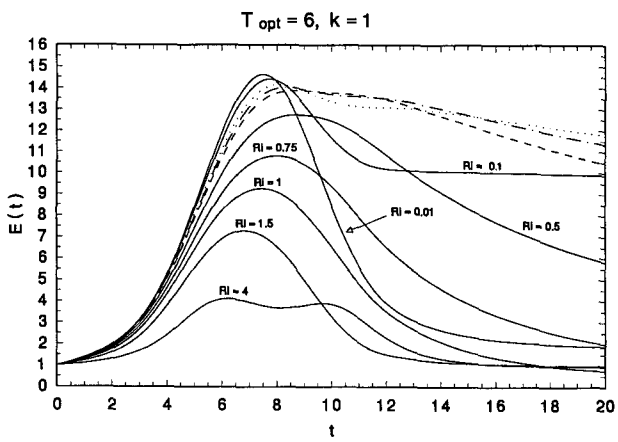

FIG. 11. Evolution of the perturbation total energy density of the optimal perturbation in the channel for $T_{opt} = 6$ and $k = 1$ as a function of time for various Ri in an unbounded shear flow. The dotted line corresponds to Ri = 0.2. The dot–dash line to Ri = 0.25 and the dashed line to Ri = 0.3. For comparison, the energy variation for the case of very small stratification Ri = 0.01 is included.

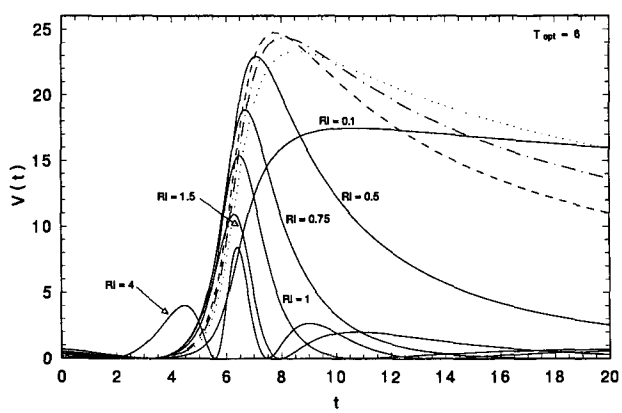

FIG. 13. Evolution of the perturbation potential energy density of the optimal perturbation in the channel for $T_{opt} = 6$ and $k = 1$ as a function of time for various Ri in an unbounded shear flow. The dotted line corresponds to Ri = 0.2. The dot–dash line to Ri = 0.25 and the dashed line to Ri = 0.3.

this Ri interval have the benefit of high-energy growth and slow decay of the potential energy [cf., (3.11)].

An example of the effect of numerical resolution on the time development of the optimal disturbance with Ri = 0.25 and $T_{opt} = 6$ is shown in Fig. 14. Convergence with 30 levels is found for a time interval of 20 advective time units. For the same problem, ten levels provide inadequate resolution. An estimate of the time interval of validity of the solution for an M-level discretization can be made by assuming that the phase speeds of the M modes are evenly distributed over the channel-flow velocities. Under this assumption, the minimum phase speed difference is in nondimensional units $1/M$. The associated frequency spread will be k/M, where k is the horizontal wavenumber. The maximum beat period of this finite set of waves $T = 2\pi M/k$ provides an approximate bound for the time interval over which the numerical solution with an M-level discretization is valid. Similar arguments have been advanced to obtain limits on the time interval of validity of models at synoptic scale (Farrell 1989). Other calculations presented in this section were performed with $M = 70$ and for $k = 1$, so that the estimated time interval of validity of the solutions extends to about 200 advective time units.

6. Discussion and conclusions

Growth and decay of perturbations in a stratified shear flow can arise, as in an unstratified flow, from exchange of kinetic energy with the mean flow mediated by the perturbation Reynolds stress. The downgradient Reynolds stress required for perturbation growth can arise either in association with exponentially growing eigenfunctions if such exist or with appropriately configured perturbations that are not in modal form. Transient energy growth from such non-

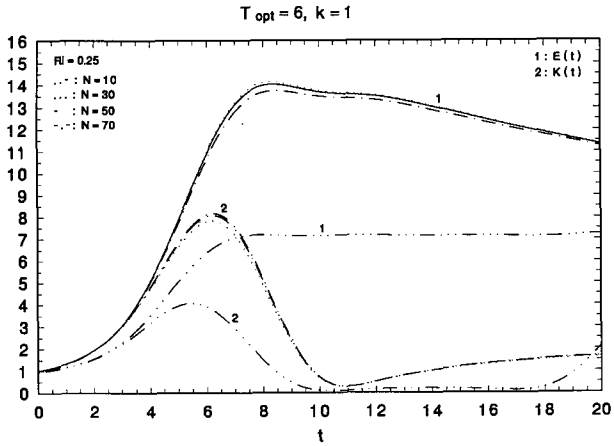

FIG. 14. Evolution of the total energy (curves 1) and kinetic energy (curves 2) for the optimal disturbance in a channel with $T_{opt} = 1$, $k = 1$ for Ri = 0.25. The various curves correspond to a different number of levels of discretization.

modal perturbations is expressed, in a modal expansion, through the nonorthogonality of the individual modes making up the perturbation. It has been shown in different circumstances (Farrell 1988a) that even when exponential instabilities are present, the initial growth of perturbations in a shear flow is dominated by the energetic interaction of the nonorthogonal modes. It follows that the study of shear-flow instability requires investigation of initial conditions capable of rapid transient energy growth. These optimally growing disturbances can be identified using a variational method that systematically reveals, from the multitude of possibilities, the most disruptive initial conditions that primarily determine the stability properties of the flow. In this work, we have limited our study to the simplest example of a stably stratified constant shear flow with constant Brunt–Väisälä frequency N^2, which is known to support no exponentially growing modes for any value of the Richardson number Ri (Goldstein 1931; Taylor 1931b). Unlike studies such as those of Eliassen et al. (1953), Case (1960), and Brown and Stewartson (1980) in which the initial value problem was used to investigate asymptotic stability of stratified shear flows in the $t \to \infty$ limit, this work focused on the potential for growth at finite times in unbounded and in bounded constant shear stratified flows.

The variational problem for determination of optimal perturbations in stratified shear flow was formulated and the role of the Ri in the development of these optimal disturbances investigated. The unbounded stratified shear flow that admits closed form solutions was studied first, and it was found that most of the salient characteristics of development are captured by this flow. It was determined that the optimally growing disturbances involve buoyancy forcing of such a phase as to initially transfer potential energy to kinetic energy in addition to the expected velocity forcing.

A basic characteristic of transient development in stratified shear flow is that the two available forms of energy, kinetic and potential, are not equipartitioned. At the early phases of development and for small Ri, kinetic energy is transferred into potential form where it decays slowly. For higher Ri, the exchange between the two forms of energy becomes more rapid, leading to reduced maximum energy amplification and more rapid decay. Causally related to this exchange between the two forms of energy is the presence of substantial buoyancy fluxes $\overline{\rho w}$, which peak near the energy maximum. This situation should be contrasted to the behavior of internal modal gravity waves in a shear flow for which energy is equipartitioned and density and vertical velocity are in quadrature leading to vanishing buoyancy flux. This modal wave behavior has encouraged adoption of a diagnostic distinction between coherent wave motions and turbulence according to whether the buoyancy flux is zero or nonzero (Itsweire et al. 1986). It is clear that care should be exercised in applying this diagnostic criterion, lest transient wave

development processes be mistaken for turbulent motion.

Turbulence in the free atmosphere is usually observed when Ri < 1, with increasing frequency of occurrence for smaller Ri (Woods 1969). The presence of exponentially growing modal disturbances, however, necessarily requires the presence of regions in the flow with Ri < 0.25 (Miles 1961; Howard 1961). The assumption that a necessary precursor to turbulence is the presence of an exponentially unstable mode, together with heuristic arguments such as that of Chandrasekhar (1961) that turbulence in a stratified flow is sustained only when Ri < 0.25 [despite the earlier estimates of Richardson (1920), Taylor (1931a), and Prandtl (1942) and the correction of Chandrasekhar's argument by Miles (1986)], led investigators to search for regions with Ri < 0.25 in order to account for observed occurrences of turbulence. We find for the development of disturbances in an unbounded shear flow and in a channel that the maximum energy attained only gradually decreases with increasing Ri, showing that the stabilizing influence of increased stratification accords no special significance to Ri = 0.25. While the maximum energy amplification is reduced with increasing Ri, asymptotically it approaches a substantial value that is equal to the square root of the the maximum amplification for unstratified flow.

While the maximum amplification shows a gradual decrease with increasing Ri, there is a remarkable phenomenon in the early development of disturbances in a flow with Ri approximately in the range 0.1 < Ri < 0.3. The transfer of perturbation kinetic energy into potential energy during the early phases of the development along with the reduced decay of transient energy for small Ri leads to enhanced persistence of perturbation potential energy when Ri lies approximately in the domain 0.1 < Ri < 0.3. This may have implications for maintenance of the perturbation variance in a stochastically driven stratified flow, suggesting enhanced variance when Ri lies in this domain.

Another remarkable feature of the development of disturbances in stratified shear flow is found when the Richardson number is less than approximately 0.4. For such Ri, even quite small initial perturbations rapidly develop locally negative stratification, implying convective instability. This suggests that transient development in shear flow at low Ri will rapidly lead to local regions of convectively generated turbulence.

Acknowledgments. Brian F. Farrell was supported by NSF ATM-8912432 and NASA through University of Maryland 26929A. Petros J. Ioannou was supported by NASA NAGW-525 and NSF ATM-9216189. Computational support for this work was provided by NCAR. The National Center for Atmospheric Research is supported by the National Science Foundation. In addition, Petros J. Ioannou thanks Richard S. Lindzen for hospitality and support at MIT.

APPENDIX

Comparison between $E(t)$ Found Using the WKB and Exact Solutions

Consider a harmonic oscillator with variable frequency Ri $\omega^2(t)$, where Ri is a large parameter. The displacement from some equilibrium position $x(t)$ satisfies

$$\frac{d^2x}{dt^2} + \mathrm{Ri}\,\omega^2 x = 0. \tag{A.1}$$

When $\omega^2(t) = (1 + t^2)^{-1}$, the motion of this oscillator corresponds to transient development of plane-wave perturbations in stratified constant shear flows with Ri identified as the Richardson number and $\sigma = 0$. For Ri $\gg$ 1, the WKB asymptotic approximation of (A.1) is obtained, which is valid to $O(1/\mathrm{Ri}^{1/2})$:

$$x(t) = x_0\left(\frac{\omega_0}{\omega}\right)^{1/2}\cos\phi + \frac{v_0}{(\mathrm{Ri}\omega\omega_0)^{1/2}}\sin\phi, \tag{A.2a}$$

$$v(t) = v_0\left(\frac{\omega_0}{\omega}\right)^{1/2}\cos\phi - x_0(\mathrm{Ri}\omega\omega_0)^{1/2}\sin\phi, \tag{A.2b}$$

where x_0 is the initial displacement, $v(t)$ is the velocity, v_0 is the initial velocity, $\omega_0 = \omega(0)$, and $\phi = \mathrm{Ri}^{1/2}\int_0^t \omega(\tau)d\tau$. The total energy E to this level of accuracy is given by

$$E(t) = \frac{\omega(t)}{2}\left(\mathrm{Ri}\omega_0 x_0^2 + \frac{v_0^2}{\omega_0}\right). \tag{A.3}$$

From (A.3), the well-known result of the adiabatic invariance of $E(t)/\omega(t)$ can immediately be seen, which implies that as ω monotonically decreases, the energy also monotonically decreases. To test the validity of the WKB approximation, (A.1) is numerically integrated with the time-dependent frequency $\omega^2(t) = (1 + t^2)^{-1}$ and the evolution of the energy amplification for Ri = 1 and Ri = 25 compared with the result from WKB analysis in Fig. A1. In Fig. A2, the corresponding

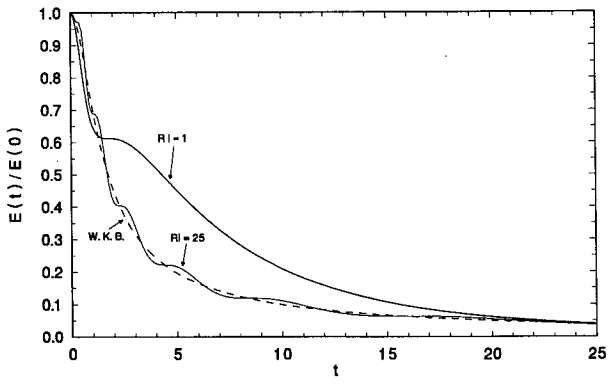

FIG. A1. Evolution of the total energy for Ri = 1 and Ri = 25. The dashed curve gives the WKB approximation, formally valid for Ri $\gg$ 1. The initial conditions were $x_0 = 1$, $v_0 = 0$.

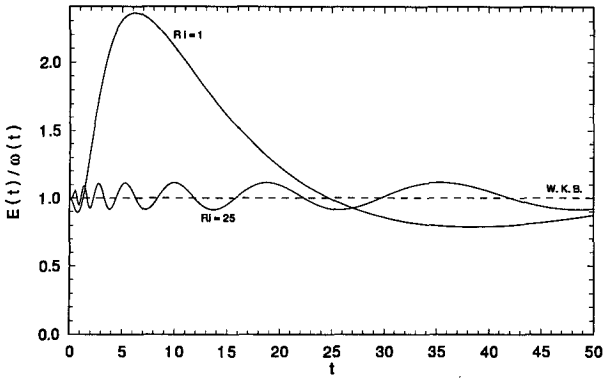

FIG. A2. Evolution of the normalized $E(t)/\omega(t)$ for Ri = 1 and Ri = 25. The dashed curve gives the WKB approximation. In the WKB approximation, the adiabatic invariant $E(t)/\omega(t)$ is a constant.

actual evolution of the WKB adiabatic invariant $E(t)/\omega(t)$ is plotted. The energy decay reveals substantial oscillations of the WKB adiabatic invariant.

Phillips (1966) considered the evolution of kinetic energy in a stratified flow with constant shear. He employed WKB analysis and obtained eventual monotonic decay of energy. Careful inspection of Figs. 3–5 shows small oscillations in the energy decay even for large Ri. This difference can be attributed to the inherent failure of second-order WKB analysis to capture these energy oscillations.

REFERENCES

Booker, J. R., and F. B. Bretherton, 1967: The critical layer for internal gravity waves in a shear flow. *J. Fluid Mech.*, **27,** 513–539.

Bretherton, F. B., 1969: Momentum transport by gravity waves. *Quart. J. Roy. Meteor. Soc.*, **95,** 213–243.

Brown, S. N., and K. Stewartson, 1980: On the algebraic decay of disturbances in a stratified linear shear flow. *J. Fluid Mech.*, **100,** 811–816.

Case, K. M., 1960: Stability of an idealized atmosphere. I Discussion of results. *Phys. Fluids,* **3,** 149–154.

Chandrasekhar, S., 1961: *Hydrodynamic and Hydromagnetic Stability.* Clarendon Press, 662 pp.

Criminale, W. O., and J. Q. Cordova, 1986: Effects of diffusion in the asymptotics of perturbations in stratified shear flow. *Phys. Fluids,* **29,** 2054–2060.

Dyson, F. J., 1960: Stability of an idealized atmosphere. II. Zeros of the confluent hypergeometric function. *Phys. Fluids,* **3,** 155–157.

Eliassen, A., and E. Palm, 1961: On the transfer of energy in stationary mountain waves. *Geofys. Publ. Oslo,* **22,** 1–23.

——, E. Hoiland, and E. Riis, 1953: Two-dimensional perturbation of a flow with constant shear of a stratified fluid. Institute for Weather and Climate Research, Norwegian Acad. of Sci. Letters, No. 1, 1.

Farrell, B. F., 1984: Modal and nonmodal baroclinic waves. *J. Atmos. Sci.*, **41,** 668–673.

——, 1988a: Optimal excitation of neutral Rossby waves. *J. Atmos. Sci.*, **45,** 163–172.

——, 1988b: Optimal excitation of perturbations in viscous shear flow. *Phys. Fluids,* **31,** 2093–2101.

——, 1989: Unstable baroclic modes damped by Ekman dissipation. *J. Atmos. Sci.*, **46,** 397–401.

——, 1990: Small error dynamics and the predictability of atmospheric flows. *J. Atmos. Sci.*, **47,** 2409–2416.

——, and P. J. Ioannou, 1993: Stochastic forcing of perturbation variance in unbounded shear and deformation flows. *J. Atmos. Sci.*, **50,** 200–211.

Fritts, D. C., 1982: Shear excitation of atmospheric gravity waves. *J. Atmos. Sci.*, **39,** 1936–1952.

——, and G. D. Nastrom, 1992: Sources of mesoscale variability of gravity waves. Part II: Frontal, convective, and jet stream excitation. *J. Atmos. Sci.*, **49,** 111–127.

Garrett, C., and W. H. Munk, 1979: Internal waves in the ocean. *Annu. Rev. Fluid Mech.*, **11,** 339–369.

Goldstein, S., 1931: On the stability of superposed streams of fluids of different densities. *Proc. Roy. Soc. A,* **132,** 524–548.

Hartman, R. J., 1975: Wave propagation in a stratified flow. *J. Fluid Mech.*, **71,** 89–103.

Hopfinger, E. J., 1973: Development of a stratified shear flow. *Proc. Int. Symp. on Stratified Flows,* Novosibirsk, USSR, Amer. Soc. Civil Eng., 553–565.

Howard, L. N., 1961: Note on a paper of John W. Miles. *J. Fluid Mech.*, **10,** 509–512.

Itsweire, E. C., K. N. Helland, and C. W. Van Atta, 1986: The evolution of grid-generated turbulence in a stably stratified fluid. *J. Fluid Mech.*, **162,** 299–338.

Joseph, D. J., 1976: *Stability of Fluid Motions I.* Springer-Verlag, 282 pp.

Kuo, H. L., 1963: Perturbations of plane couette flow in stratified fluid and origin of cloud streets. *Phys. Fluids,* **6,** 195–211.

Lilly, D. K., 1972: Wave momentum flux. A GARP problem. *Bull. Amer. Meteor. Soc.*, **53,** 17–23.

Lindzen, R. S., 1990: *Dynamics in Atmospheric Physics.* Cambridge University Press, 310 pp.

Long, R. R., 1953: Some aspects of the flow of stratified fluids. I. A theoretical investigation. *Tellus,* **5,** 42–58.

Miles, J. W., 1961: On the stability of heterogeneous shear flows. *J. Fluid Mech.*, **10,** 496–508.

——, 1986: Richardson's criterion for the stability of stratified shear flow. *Phys. Fluids,* **29,** 3470–3471.

Nastrom, G. D., and D. C. Fritts, 1992: Sources of mesoscale variability of gravity waves. Part I: Topographic excitation. *J. Atmos. Sci.*, **49,** 101–110.

Phillips, O. M., 1966: *The Dynamics of the Upper Ocean.* 1st ed. Cambridge University Press, 336 pp.

Prandtl, L., 1942: *Führer durch die Strömungslehre.* Braunschweig, 337 pp.

Queney, P., 1948: The problem of air flow over mountains: A summary of theoretical studies. *Bull. Amer. Meteor. Soc.*, **29,** 16–26.

Richardson, L. F., 1920: The supply of energy from and to atmospheric eddies. *Proc. Roy. Soc. A,* **97,** 354–373.

Sawyer, J. S., 1959: Introduction of the effects of topography into methods of numerical weather forecasting. *Quart. J. Roy. Meteor. Soc.*, **85,** 31–43.

Scorer, R. S., 1949: Theory of waves in the lee of mountains. *Quart. J. Roy. Meteor. Soc.*, **75,** 41–56.

——, 1955: Theory of air flow over mountains. IV. Separation of flow from the surface. *Quart. J. Roy. Meteor. Soc.*, **81,** 340–350.

Stull, R. B., 1976: Internal gravity waves generated by penetrative convection. *J. Atmos. Sci.*, **33,** 1279–1286.

Taylor, G. I., 1931a: Internal waves and turbulence in a fluid of variable density. *Rapp. P. V. Reun. Cons. Int. Explor. Mer,* Sci. Pap. **2,** 240–246.

——, 1931b: Effect of variation in density on the stability of superposed streams of fluid. *Proc. Roy. Soc. A,* **223,** 499–523.

Thorpe, S. A., 1987: Transitional phenomena and the development of turbulence in stratified fluids: A review. *J. Geophys. Res.*, **92,** 5231–5248.

Turner, J. S., 1979: *Buoyancy Effects in Fluids.* Cambridge University Press, 368 pp.

Woods, J. D., 1969: On Richardson's number as a criterion for laminar—turbulent—laminar transition in the ocean and atmosphere. *Radio Sci.*, **4,** 1289–1298.